Talanta 112 (2013) 129–135

Contents lists available at SciVerse ScienceDirect

Talanta

journal homepage: www.elsevier.com/locate/talanta

Electrophoresis deposition of Ag nanoparticles on TiO_2 nanotube arrays electrode for hydrogen peroxide sensing

Yanshu Jiang [a], Baozhan Zheng [a], Juan Du [a], Guangyue Liu [a], Yong Guo [a], Dan Xiao [a,b,*]

[a] College of Chemistry, Sichuan University, 29 Wangjiang Road, Chengdu 610064, PR China
[b] College of Chemical Engineering, Sichuan University, 29 Wangjiang Road, Chengdu 610065, PR China

ARTICLE INFO

Article history:
Received 24 December 2012
Received in revised form
4 March 2013
Accepted 5 March 2013
Available online 13 March 2013

Keywords:
TiO_2 nanotube arrays
AgNPs/TiO_2NTs
Electrophoretic deposition
Hydrogen peroxide sensor

ABSTRACT

In this paper, a simple and green strategy, based on the electrophoresis deposition technology, was reported to prepare Ag nanoparticles (NPs) modified TiO_2 nanotube arrays (NTs). The morphologies of AgNPs, TiO_2NTs and AgNPs/TiO_2NTs were characterized by transmission electron microscope (TEM) and scanning electron microscope (SEM). The results demonstrate that the surface of TiO_2NTs was homogeneously decorated with AgNPs, of which the morphology could be easily controlled by the electrophoretic deposition (EPD) time. In order to investigate the co-effects of AgNPs and TiO_2NTs on the catalysis of H_2O_2, the electrochemical performances of TiO_2 NTs, AgNPs/Ti and AgNPs/TiO_2NTs electrodes were investigated in this work. It is found that the response of AgNPs/TiO_2NTs electrode to H_2O_2 was remarkably enhanced due to the co-effects of AgNPs and TiO_2NTs. Therefore, it could be used to fabricate H_2O_2 sensor. The effects of conditions were investigated in detail, such as EPD time, the operating potential, etc.. Under the optimal experimental condition, the sensor had a quick response to H_2O_2 at −0.12 V with a high sensitivity (184.24 $mA{\cdot}M^{-1}\ cm^{-2}$), wide linear range (0.75 μM–11.16 mM) and low detection limit (85.6 nM). In addition, the sensor also has good stability and excellent selectivity. The developed H_2O_2 sensor has been successfully applied to the detection of H_2O_2 in real samples. This work also demonstrated that the AgNPs/TiO_2NTs has potential application in fabricating glucose sensor by immobilizing glucose oxidase onto the prepared electrode.

1. Introduction

The stable hydrogen peroxide (H_2O_2) sensors with high sensitivity, low detection limit and wide linear range have been studied extensively in the areas of food [1], pharmaceutical [2] and environmental analyses [3,4]. This has led to the development of spectrometry [5], chemiluminescent [6] and electrochemical sensors [7–9] for the detection and quantification of H_2O_2. Among these, electrochemical methods are superior for their relatively low cost, high efficiency, high sensitivity and the ease of operation [10,11]. Many noble metal nanoparticles (NPs), such as PtNPs [7], AuNPs [12], AgNPs [13] and PdNPs [14] have been widely used in electrochemical detectors, owing to their excellent conductivity, extraordinary electrocatalytic property and larger specific surface area [15]. Among these materials, the conductivity of silver is the best and the price is much cheaper than the other noble metal mentioned above. Furthermore, the AgNPs show excellent electrocatalytic activity to H_2O_2 [16], therefore, it is the suitable metal nanoparticles for H_2O_2 sensor fabrication. Recent studies [15,17,18] indicate that the shape and the distribution of AgNPs played a vital role in the catalytic process to H_2O_2 and the substrate material for the loading of AgNPs is also very important to the fabrication of sensors with higher performance.

The supported system has a major influence on fabricating a nanostructured AgNPs modified sensor with higher sensitivity and reproducibility. Many metal oxides, such as Al_2O_3, SiO_2, TiO_2, etc. are common substrate materials used for electrodes' fabrication. Among them, the highly ordered TiO_2 nanotubes (NTs) have good biocompatibility, large surface area, excellent electron-transfer behavior and large numbers of active reaction sites for chemical reactions [19–22]. Therefore, TiO_2NTs can be regarded as an ideal substrate material to fabricate sensors. In the process of modifying TiO_2NTs electrode by metal nanoparticles, the key point for nanoparticles coating is the control of the size and/or shape of nanoparticles as well as their self-assembly within ordered structures, which is also a great challenge in the current nanofabrication technology due to the small dimensions of nanomaterials [23,24]. On account of the wide usage of AgNPs/TiO_2NTs in the field of photocatalysis [25,26], bactericides [27], lithium-ion battery [28], dye-sensitized solar cells [29] and sensors (gas sensor [30], humidity sensor [31] and polycyclic aromatic hydrocarbons

* Corresponding author at: College of Chemistry, Sichuan University, 29 Wangjiang Road, Chengdu 610064, PR China. Tel.: +86 28 85416029; fax: +86 28 85415029.
E-mail address: xiaodan@scu.edu.cn (D. Xiao).

0039-9140/$ - see front matter © 2013 Elsevier B.V. All rights reserved.
http://dx.doi.org/10.1016/j.talanta.2013.03.015

sensor [32]), some methods have been employed to prepare AgNPs/TiO_2NTs, including microwave-assisted approach [25], electrodeposition [33,34], chemical reduction method [28] and photodeposition [33]. However, most of the existing techniques involve the use of toxic additives. In addition, the deposition process is difficult to be controlled, thus invariably leading to unordered particles aggregation on the top of nanotubes.

Herein, a straightforward strategy to overcome these problems is proposed, which mainly bases on the conventional electrophoretic deposition (EPD) techniques. The mechanism of EPD is that the charged particles will be driven to and then deposited on the surface of the substrate when an electric field is applied perpendicular to the substrate [35]. Then a regular morphology of the modified electrode with high conductivity could be obtained by EPD techniques, therefore it has attracted significant attention in the last two decades for various applications. For example, TiO_2 NPs that deposited on a membrane of Ag fibers by EPD was employed as a photoelectrochemical cell electrode [36], hydrothermally synthesized Ag–TiO_2 hybrid NPs were deposited onto 3-D Ni-based filters by EPD so that a fully coated morphology was obtained [37], Au nanoparticle-decorated ZnO nanorod arrays were fabricated by electrophoresis and exhibited excellent surface-enhanced Raman scattering performance [38]. In the above reports, nanopaticles are modified on the outside surface of substrate materials, however, there were few reports that deposited nanoparticles on both inside and outside surface of the TiO_2NTs by electrophoresis to fabricate sensors.

In this work, a facile EPD technology was used to synthesize AgNPs modified TiO_2NTs. The prepared AgNPs rapidly deposited on the walls of TiO_2NTs under the electric field. By adjusting the voltage and time of electrophoresis, the aggregation of AgNPs on the surface of TiO_2NTs could be prevented, which ensured large specific surface area of the electrodes, and led to a higher sensitive sensor. The electrochemical catalytic activity of the as-prepared AgNPs/TiO_2NTs electrode to H_2O_2 was investigated in detail. The results show that the AgNPs/TiO_2NTs electrode has a better response to H_2O_2 than the single-component TiO_2NTs and AgNPs/Ti electrodes, therefore it could be used as a non-enzymatic H_2O_2 sensor. In addition, the AgNPs/TiO_2NTs fabricated by EPD also have a low detection limit and wide responding range to H_2O_2. Besides, the as-prepared H_2O_2 sensor could also be used to detect H_2O_2 in disinfectant and satisfactory results were obtained, which demonstrated that AgNPs/TiO_2NTs has a potential application in real sample detection.

2. Experimental

2.1. Reagents and materials

Ammonium fluoride (NH_4F) and silver nitrate ($AgNO_3$) were obtained from Chengdu Chemicals (Chengdu, China), gallotannin acid was obtained from Beijing Chemical Works (Beijing, China), and glycerol was from Meilin Industry and Trade Co., Ltd. (Tianjin, China). Potassium carbonate and hydrogen peroxide (30%, w/w in water, 99% purity) were purchased from Kelong Chemical Reagent Company (Chengdu, China). The solution of H_2O_2 was prepared before use to avoid excessive decomposition. Phosphate buffer solutions (PBS) were prepared by mixing stock standard solutions of Na_2HPO_4 and NaH_2PO_4. All chemicals were of analytical grade and used as received. Double-distilled water was used throughout the experiments.

2.2. Synthesis of TiO_2NTs

Highly ordered TiO_2NTs were fabricated by electrochemically anodizing Ti foils (200 μm thick, 99.6% purity) in a fluoride-containing glycerol electrolyte [39]. Briefly, all anodizations were carried out by using the self-designed equipment consisting of two pieces of Ti foils as cathodes and a piece of Ti foil as anode. The distance between the anode and each cathode was about 30 mm. All Ti foils were ultrasonically cleaned orderly with acetone, isopropanol and double-distilled water, and then dried in air prior to use. The cleaned Ti foil was anodized in a 100 mL glycerol solution containing 1 wt% NH_4F and 10 vol% H_2O (i.e., 10 mL of H_2O and 90 mL of glycerol). All the experiments were carried out at room temperature, the anodization process was performed with a DC stabilized power supply (QF1723M, State Qianfeng Radio Instrument Factory) and consisted of a potential sweep from 0 V to 50 V at a rate of 2 V min^{-1}, followed by holding the potential at 50 V for 3 h. After anodization, the anodized Ti foils were rinsed with double-distilled water and dried in air. To improve the crystalline properties and mechanical stability, the anodized Ti foils were annealed at 400 °C for 2 h under ambient atmosphere.

2.3. Electrophoretic deposition

Electrophoretic deposition experiments were carried out using a microcomputer-based Autolab electrochemical workstation (PGSTAT 30/302, Netherlands) connected to a three-electrode cell at room temperature. Two Pt foil counter electrodes and an SCE (Saturated Calomel Electrode, saturated by KCl) were used in the three-electrode system. The EPD cell used in this work was a 50 mL glass beaker, the TiO_2NTs was used as the working electrode and immersed into 40 mL AgNPs colloid solution, the distance between working electrode and each counter electrode were 1.5 cm, as illustrated in Scheme 1. Chronoamperometry was performed for 15–35 min at an operating voltage of −0.4 V. The liquid phase was vigorously stirred with a magnetic stirrer during the process of deposition. After the electrophoresis, the TiO_2NTs electrode, which became yellow-brown, was softly rinsed with double-distilled water, and dried in a stream of N_2 before characterization.

2.4. Instruments

X-ray diffraction (XRD) measurements were performed on a Tongda TD-3500 X-ray powder diffractometer (Liaoning, China) with Cu Kα radiation (λ=0.154 nm). The XRD patterns were recorded from 20° to 80° at a scan rate of 0.03° s^{-1}. The morphology of AgNPs/TiO_2NTs was analyzed by field-emission scanning electron microscope (FESEM, Hitachi S-4800, Japan) and transmission electron microscope (TEM, JEM 100CX II, Japan). Cyclic voltammetry (CV), chronoamperometry and electrochemical impedance (EIS) were performed using a potentiostat/galvanostat Autolab (PGSTAT 30/302, Netherlands) electrochemical analyzer system. A conventional three-electrode cell was used, AgNPs/TiO_2NTs (1 cm × 1 cm), SCE(Saturated Calomel Electrode) electrode

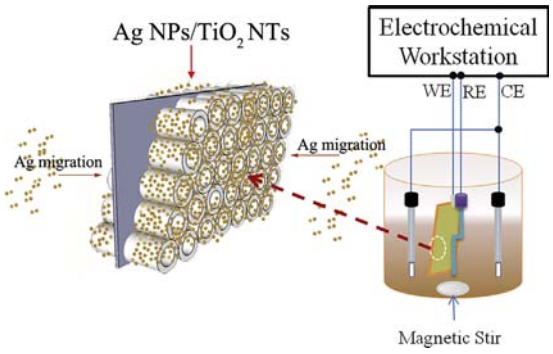

Scheme 1. Schematic illustration for the surface decoration strategy of TiO_2NTs based on electrophoresis deposition in the Ag colloidal solution.

and platinum wire were used as working electrode, reference electrode(saturated by KCl) and counter electrode, respectively. All potentials given in this work were referred to the SCE electrode and all the experiments were carried out at ambient temperature.

3. Results and discussion

3.1. Material characterization

The surface morphology of the synthesized TiO_2NTs and AgNPs/TiO_2NTs was characterized by FESEM. The FESEM image of as-prepared TiO_2NTs is shown in Fig. 1(A). It is observed that the prepared materials consists of regular tubes with a diameter of 145 ±5 nm and a wall thickness of 15±2 nm. It can be inferred that the diameter is large enough to allow AgNPs(the size distribution of AgNPs is shown in Fig. S1) enter the tubes during the electrophoretic deposition process. Therefore, AgNPs were presented not only on the top surface (see Fig. 1(B)) but also on the internal surface (see Fig. 1(E) and (F)) of TiO_2NTs. The effect of EPD time on the morphology of AgNPs/TiO_2NTs was also investigated by FFSEM. Fig. 1(B–D) shows the images of the AgNPs/TiO_2NTs with different EPD time. From the results it can be seen that the AgNPs deposition process does not damage the ordered array structure of TiO_2NTs, and AgNPs have been successfully deposited on the surface of TiO_2NTs, the XRD patterns in Fig. S2 indicate the existence of silver. It also reflects that the applied potential (−0.4 V) is high enough so that the charged AgNPs in the colloidal solution could be quickly driven to the TiO_2NTs electrode.

When the EPD time is 15 min, the AgNPs could be deposited on the top, inside and outside surfaces of the TiO_2NTs walls and their size is the same as they are in the fresh AgNPs colloid solution (the TEM image of the fresh AgNPs is shown in Fig. S1). However, there are still a few AgNPs about 20 nm appeared near the edge of nanotubes (see in Fig. 1(B)). This could be explained by that the moving AgNPs colloids would grow up after a long time deposition before reaching the array's surface, the mechanisms for the crystal growth could be explained by Ostwald ripening [40–42], which involves the growth of larger crystals with the expense of smaller crystals. Consequently, the size of AgNPs in the colloid solution significantly increased after 25 min of EPD. Due to the stronger effect of electric field around the edges or corners of each nanotubes, most of the grown-up particles deposited on the top of the nanotubes and a few of them could enter the nanotubes' channel. Fig. 1(E) depicts the TEM image of TiO_2NTs with some grown-up AgNPs deposited. Except the large size of AgNPs, there are still large numbers of small AgNPs (about 1–2 nm) attached to the walls of TiO_2NTs(shown in Fig. 1(F)). When the EPD time is 35 min, the AgNPs in the colloidal solution grew into bigger ones and deposited on the top of nanotubes under the electric field.

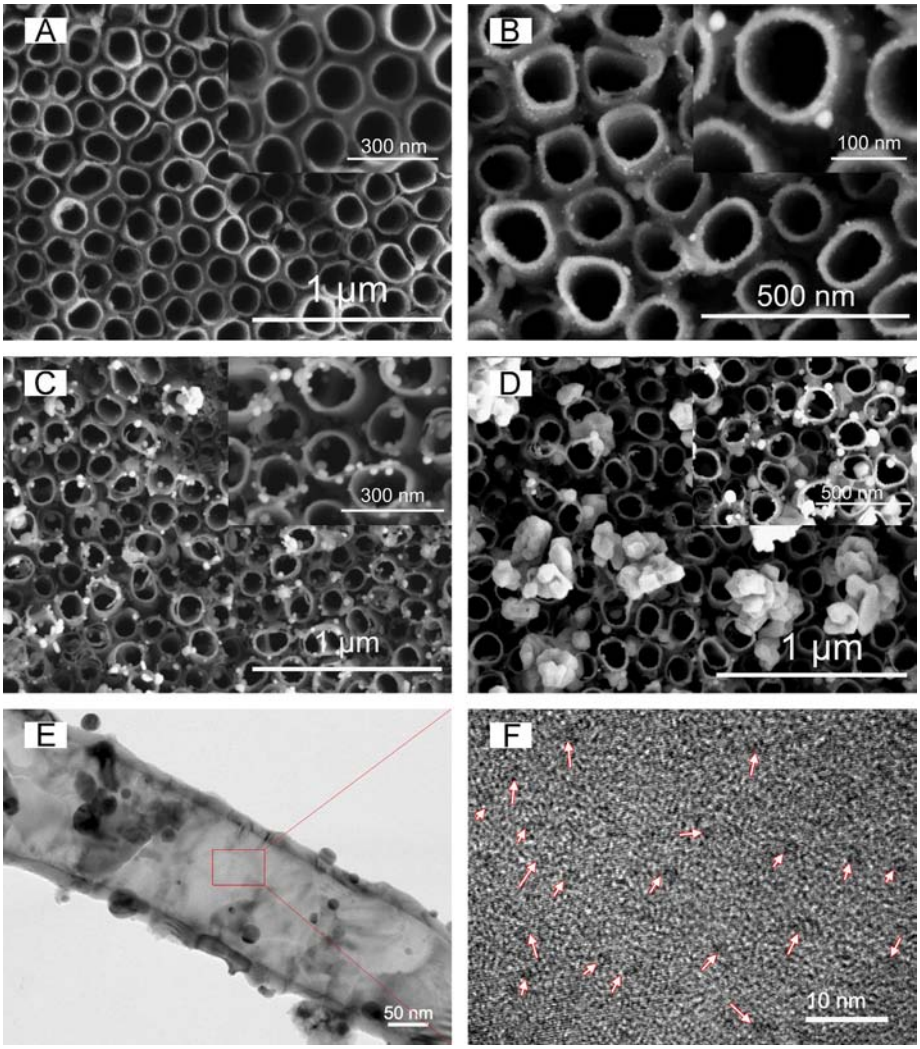

Fig. 1. The FE-SEM images of TiO_2NTs (A) and AgNPs/TiO_2NTs, prepared with various deposition times (B) 15 min, (C) 25 min and (D) 35 min, (E) TEM images of Ag/TiO_2NTs (deposition time: 25 min), (F) is the HRTEM images of the areas marked by red rectangle in (E).

Fig. 1(D) shows that some particles are larger than 100 nm which even could block the TiO_2 NT mouths, resulting in a decrease in the specific surface area of the TiO_2NTs.

3.2. Electrochemical performance of the AgNPs/TiO_2NTs electrode

Cyclic voltammetry is employed to characterize the electrochemical behavior of the electrode. Fig. 2(A) shows the CV curves of AgNPs/TiO_2NTs electrode(curve b) and a blank TiO_2NTs electrode(curve a) in 0.1 M PBS (pH 7.4). From the results, neither reduction nor oxidation peak were observed on TiO_2NTs electrode. In contrast, AgNPs/TiO_2NTs electrode showed two couples of well-defined redox peaks which appeared at −0.44 V and −0.12 V (for the first couple) and −0.09 V and 0.38 V (for the other couple), respectively (Fig. 2(A), curve b). The two couples of redox peaks come from the two states of the immobilized AgNPs, which occurring at lower potential were assigned to the redox of AgNPs anchored in the internal walls of the nanotubes, and another couple of redox peaks resulted from the redox of the AgNPs adsorbed on the top surface of the nanoporous structure by EPD deposition, similar result was also reported in the study of immobilized Hb [43] on nanoporous TiO_2 films. Therefore, the redox peaks of curve b in Fig. 2(A) also demonstrate the existence of silver particles on the surface of TiO_2NTs.

The electrochemical response of the TiO_2NTs and AgNPs/TiO_2NTs electrode to H_2O_2 was investigated in this work. Fig. 2 (B) shows the CVs of TiO_2NTs (curve a) and AgNPs/TiO_2NTs (curve b) electrode in the presence of 1mM H_2O_2. Compared with TiO_2NTs electrode, the AgNPs/TiO_2NTs electrode exhibited excellent response to H_2O_2. In order to study the effects of TiO_2NTs in the system, the behavior of AgNPs/Ti, prepared by depositing AgNPs on the surface of Ti substrate, was also studied. The electrochemical behavior of AgNPs/Ti electrode was shown in Fig. 2(C). As Fig. 2(C) shows, a much weaker electrocatalytic response to H_2O_2 at about −0.12 V is found (curve b) on the AgNPs/Ti electrode, which is much lower than that on the AgNPs/TiO_2NTs (Fig. 2(B), curve b) at the same conditions. This demonstrates that the TiO_2NTs can serve as not only a substrate for AgNPs loadding, but also unblocked “nanochannels”, which can allow H_2O_2 to enter the nanotubes more easily and have more chances to react with the anchored AgNPs.

From the results, the reduction of H_2O_2 could be occured at both −0.4 V and −0.12 V, and the response current at −0.4 V is stronger than that at −0.12 V(Fig. 2(B) curve b), the drastic enhancement of the reduction current at about −0.4 V corresponds to the irreversible reaction of H_2O_2 on the surface of TiO_2NTs [44–46]. As is shown in Fig. S4, cathode peak current of the AgNPs/TiO_2NTs electrode which has been used for the detection of H_2O_2 is obviously different from the newly prepared AgNPs/TiO_2NTs electrode at about −0.4 V in the PBS solution, but almost the same at about −0.12 V. It can be inferred that when AgNPs/TiO_2NTs electrode was used to amperometric detect H_2O_2 at an applied potential of −0.4 V, it could not be used repeatedly because of the background current could not recovery to the original current value. However, other reducible species may interfere the detection of H_2O_2 at −0.4 V (see Table S1), such as UA, glucose, DA etc. It has been reported that the interference can be significantly reduced at a relatively low applied potential [11]. In order to enhance the selectivity of the sensor, the potential of −0.12 V was chosen as the optimum detection potential in the following detection experiments.

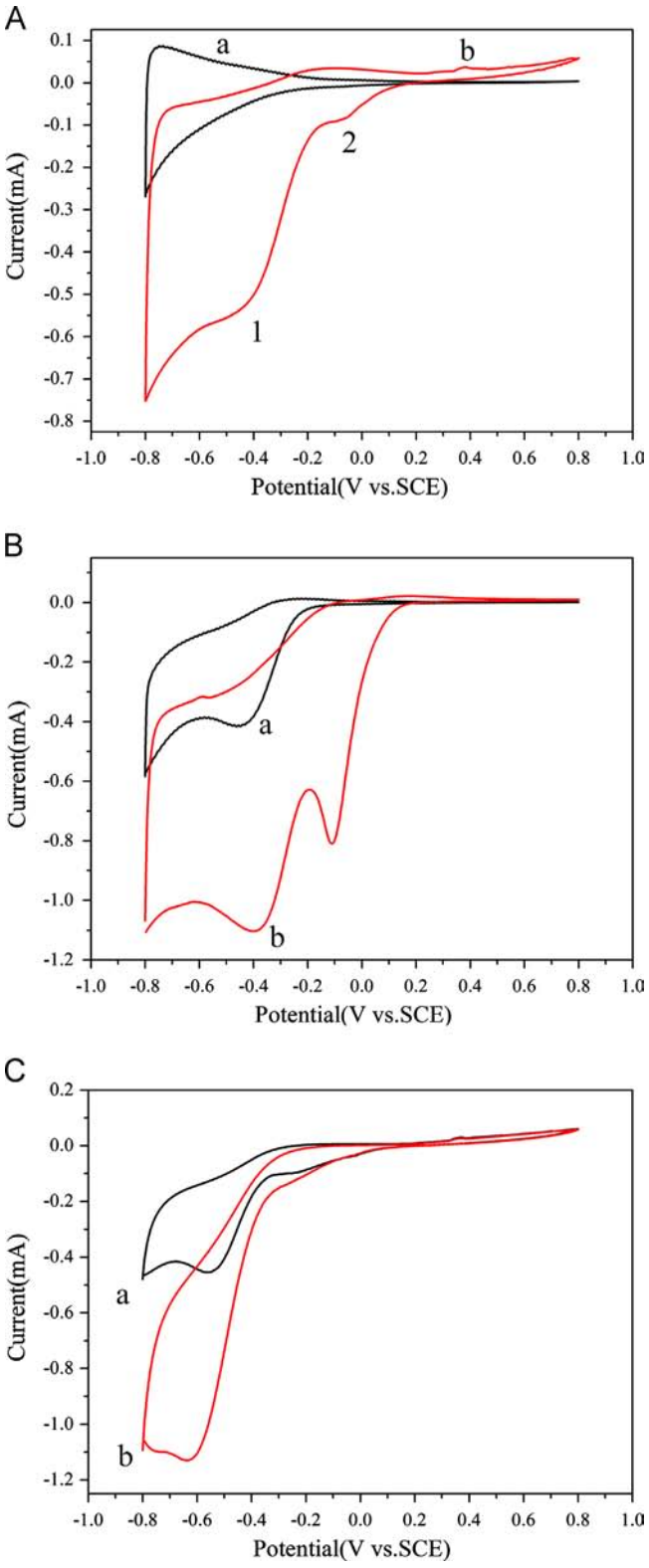

Fig. 2. (A) Cyclic voltammograms (CVs) of TiO_2NTs (a) and AgNPs/TiO_2NTs (b) electrodes in 0.1 M PBS (pH 7.4). (B) CVs of TiO_2NTs (a) and AgNPs/TiO_2NTs (b) electrode in the presence of 1 mM H_2O_2 in 0.1 M PBS (pH7.4). (C) CVs of the AgNPs/Ti electrode in the absence (a) and presence (b) of 1 mM H_2O_2 in 0.1 M PBS (pH7.4). Scan rate: 50 mV s^{-1}.

3.3. The optimization of the electrophoretic deposition time

The amount of AgNPs on the surface of TiO_2NTs, mainly depended on the EPD time, could affect the current response of the electrode to H_2O_2. Fig. 3 shows the calibration plot of response current of AgNPs/TiO_2NTs electrodes prepared with various deposition time (15–35 min) against H_2O_2 concentration. The inset shows the effect of EPD time on the sensitivity of AgNPs/TiO_2NTs

electrodes to H_2O_2. It can be seen that the sensitivity of the electrode to H_2O_2 increased as the EPD time increased and reached a maximum at 25 min, which could ascribed to the large number of highly dispersed small AgNPs on the electrode. When the EPD time is more than 25 min, the response current decreased slightly. This might be due to the fact that AgNPs would become bigger with the excessive EPD time, as illustrated in Fig. 1(D), and the bigger particles would block the channels of TiO_2NTs and thus decrease the electrocatalytic sites on the AgNPs/TiO_2NTs electrode. Therefore, 25 min was selected as the optimal EPD time for the deposition of AgNPs in further experiments.

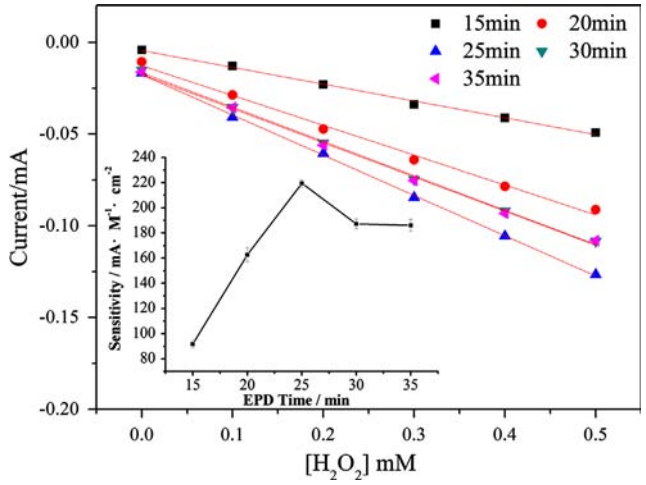

Fig. 3. The calibration plot of response current of AgNPs/TiO_2NTs electrodes to H_2O_2 prepared with various deposition time (15–35 min) against hydrogen peroxide concentration. The inset shows the sensitivity of AgNPs/TiO_2NTs electrodes to H_2O_2 against EPD time.

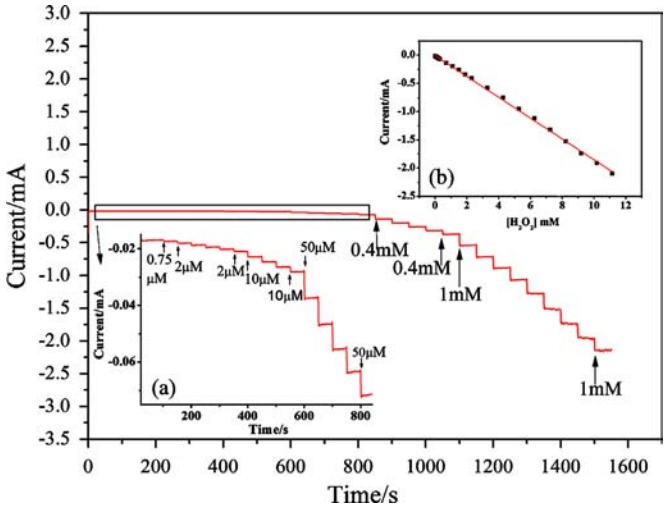

Fig. 4. Typical amperometric current responses of AgNPs/TiO_2NTs electrodes (deposition time: 25 min) upon successive additions of H_2O_2 at an operating potential of −0.12 V in 0.1 M PBS (pH7.4). Inset (a) is the enlarged amperometric current response of the areas marked by black rectangles. Inset (b) is the calibration plot of response current against hydrogen peroxide concentration.

3.4. Analytical performance of the H_2O_2 sensor and sample analysis

Fig. 4 shows the amperometric response of AgNPs/TiO_2NTs electrode to successive additions of H_2O_2 at a constant potential of −0.12 V in 0.1 M PBS (pH 7.4), and it exhibited a rapid response to H_2O_2. Inset (b) exhibits the plot of response current of AgNPs/TiO_2NTs electrode against H_2O_2 concentration. It can be seen from inset (b) that the sensor has a good linear current response to H_2O_2 ranging from 0.75 μM to 11.16 mM with a correlation coefficient of 0.9989. The detection limit of the sensor to H_2O_2 is 85.6 nM ($S/N=3$). Compared with other reported sensors, the proposed sensor has a high sensitivity (184.24 mA M^{-1} cm^{-2}) and a fast response time to H_2O_2(less than 5 s), this should be attributed to the AgNPs deposited onto the nanotubes, which could enhance the conductivity of TiO_2NTs and promote the direct electron transfer. In order to prove the effects of AgNPs, the response of TiO_2NTs electrode without AgNPs deposited to H_2O_2 was also investigated, the result (shown in Fig. S5) indicates that the current response of TiO_2NTs electrode is much smaller than that of the AgNPs/TiO_2NTs electrode. Therefore, we can conclude that the high sensitivity and fast response to H_2O_2 should be assigned to the synergistic effects of AgNPs and TiO_2NTs.

The reproducibility and stability are very important for the sensor applied to detect some real samples. Therefore, the reproducibility and stability of the proposed H_2O_2 sensor was evaluated by measuring its response to 0.1 mM H_2O_2 at −0.12 V. In this case, eight electrodes were prepared at the same conditions, were selected to detect H_2O_2 and a R.S.D. of 4.6% was obtained, confirming that the fabrication method was highly reproducible. In addition, twenty successive amperometric measurements at one modified electrode yielded a reproducible current with a R.S.D. of 4.8%, indicating that the sensor was stable and could be used repeatedly for the detection of H_2O_2 without poisoned by the oxidation products. The sensor drift was calculated by testing the response current decay rate of the Ag/TiO_2NTs electrode, the response current could be maintained 96% of its initial within 1000s after adding H_2O_2 (see Fig. S6), indicating that the Ag/TiO_2NTs hybrid structure possesses good tolerance against reaction intermediates and may be applicable for long-term application. The long-term stability of the sensor was also evaluated. The sensor was stored in air at ambient conditions and its sensitivity to H_2O_2 was tested every 10 days. The result demonstrated that the response current retained 97.5% of its initial response current after being stored for 60 days (See Fig. S7). The good reproducibility and long-term stability of the prepared H_2O_2

Table 1
Performance comparison of the proposed sensor for hydrogen peroxide detection with other sensors. (NPs=nanoparticles, NRs=nanorods, G=graphite, F=functional, GO= graphene oxide, GC=glassy carbon, NTs=nanotubes).

Type of the electrode	Applied potential (V)	LOD (μM)	Linear range (mM)	Stability	References
Ag-3D catalyst/G	0.6	1.0	0.05–2.5	92% remains after 30 days	[10]
AgNPs/ZnONRs/FTO	−0.55	0.9	0.008–0.983	–	[15]
AgNPs/GC	–	2	–	–	[16]
AgNPs/ATP/GC	−0.3	2.4	0.015–21.530	No obvious change after 14 days	[17]
AgNPs/DNA/GC	−0.4	1.7	0.004–16	No obvious change after 30 days	[18]
AgNPs/type I collagen/GC	0.3	0.7	0.005–40.6	No obvious change after 30 days	[47]
AgNP/F-SiO_2/GO/GC	−0.3	4	0.1–0.260	92.9% remains after 5 days	[48]
AgNPs/TiO_2NTs	−0.12	0.0856	0.00075–11.16	97.5% remains after 60 days	This work

sensor are desirable for most routine analysis. A comparison of applied potential, sensitivity, LOD (limit of detection), linear range, detection limit, and stability for this AgNPs/TiO_2NTs modified electrode with other hydrogen peroxide sensors reported was shown in Table 1. It can be seen that our AgNPs/TiO_2NTs H_2O_2 sensor performs better.

One of the most important analytical factors for an amperometric sensor is its ability to discriminate the interfering species having electroactivities similar to the target analyte. To investigate whether the sensor is specific for H_2O_2, common interferences were studied under the same conditions by calculating the ratio of response current (I_s/I_0). I_s and I_0 were chronoamperometric response current of H_2O_2 at −0.12 V in the presence and absence of other compounds. As shown in Table 2, no obvious current changes were observed in the presence of other interference. Response current ratio only slightly varied from 0.92 to 1.07 in the presence of some possible interfering substances including Ca $(NO_3)_2$, KCl, Na_2SO_4, DA, UA, AA and D-(+)-glucose. The above results indicate that our sensing system has a high selectivity toward H_2O_2 with the presence of other interferences. This excellent selectivity should be attributed to the unique reaction between the H_2O_2 and AgNPs/TiO_2NTs, as discussed above.

To illustrate the feasibility of the H_2O_2 sensor in practical analysis, it was employed to measure the H_2O_2 content in H_2O_2 disinfectant from different manufacturers. The samples were diluted 2000 folds by a 0.1 M PBS buffer (pH 7.4). The H_2O_2 content was determined by the standard addition method. Table 3 displays the results obtained from the proposed sensor and a titrimetry method. The recovery tests for H_2O_2 were performed by adding different volume of H_2O_2 in the sample solutions. The amounts of added H_2O_2 were then evaluated by using the proposed H_2O_2 sensor. The results of recovery test are summarized in Table 2. These results demonstrate that our proposed H_2O_2 sensor offers an excellent and accurate method for H_2O_2 determination.

Table 2
Amperometric responses current ratio (I_s/I_0) of AgNPs/TiO_2NTs electrodes to 1×10^{-3} M H_2O_2 with the conexistence of other interfering substance at a concentration of 1×10^{-3} M. Operating potential: −0.12 V.

Interferent	I_s (current/μA)	Ratio of response current (I_s/I_0[a])
$Ca(NO_3)_2$	−18.75	0.94
KCl	−18.28	0.92
Na_2SO_4	−19.19	0.96
DA	−20.71	1.04
UA	−21.36	1.07
AA	−20.41	1.02
D-(+)-glucose	−20.35	1.02

[a] I_0 was −19.86 μA.

3.5. Detection of glucose at the GOx–AgNPs/TiO_2NTs electrode

As we know that the quantified determination of glucose with a glucose sensor is mainly based on the electrochemical detection of the enzymatically liberated H_2O_2, and the sensitivity of the sensor is dependent on the electrochemical response of the sensor to H_2O_2, electrodes with high catalytic efficiency to H_2O_2 could also enhance the sensitivity of the sensor to glucose [49]. To investigate the sensing ability of sensor to glucose, the glucose oxidase (GOx) was immobilized on the surface of AgNPs/TiO_2NTs (GOx–AgNPs/TiO_2NTs). The CV measurements of GOx–AgNPs/TiO_2NTs electrode were carried out in an air-saturated PBS solution containing different concentrations of glucose (0–800 μM glucose) (Fig. 5). It can be seen that the electrocatalytic response of the electrode to H_2O_2 at about −0.12 V increases with the increasing of glucose concentration. At the same time, the reductive current at the FAD redox potential (−0.31 V) gradually decreases with the increasing of glucose concentration, the response of the electrode to glucose at −0.31 V exhibiting two linear regions of glucose concentration, respectively in 20–200 μM (R=0.9991) and 200–800 μM (R=0.9917). The corresponding sensitivities of the glucose sensor are 248.55 μA mM^{-1} cm^{-2} and 99.27 μA mM^{-1} cm^{-2}, respectively, which are both much more sensitive than other methods reported [21]. As the above discussion, the prepared GOx–AgNPs/TiO_2NTs glucose sensor also has a potential application in the determination of glucose.

4. Conclusions

In summary, a densely packed TiO_2NTs was synthesized based on the anodic oxidation method and AgNPs/TiO_2NTs electrode was then prepared by depositing AgNPs on the surface of TiO_2NTs with EPD technique, and its application for amperometric detection of H_2O_2 was investigated. Compared with AgNPs/Ti electrode and TiO_2NTs electrode, the AgNPs/TiO_2NTs electrode exhibited higher catalytic activity toward H_2O_2 at −0.12 V. The study results show that the presence of AgNPs and TiO_2NTs were both responsible for the greatly enhanced performance of the sensor. The morphology of AgNPs loaded on TiO_2NTs and the sensitivity of the electrode to H_2O_2 could be controlled by changing the EPD time. The proposed H_2O_2 sensor with high sensitivity and low detection limit mainly depended on a key factor: the highly dispersed AgNPs decorated TiO_2NTs prepared by EPD technology. Satisfyingly, the fabricated AgNPs/TiO_2NTs could not only be applied to construct a H_2O_2 sensor, but also be used for preparation of glucose sensor via immobilizing GOx onto the AgNPs/TiO_2NTs electrode. Such AgNPs/TiO_2NTs nanocomposites may possess great prospect for applications in areas including environment, analytical chemistry and clinical medicine.

Table 3
Determination of H_2O_2 contents in real samples using the proposed H_2O_2 sensor and titrimetry method, and recovery test for real sample.

Sample[a]	Conc. (H_2O_2) in disinfectant (M)			Concentration of H_2O_2 added (mM)	Concentration of H_2O_2 found (mM)[b]	Recovery (%)
	Proposed method[b]	Titrimety method	R.S.D.[b,c] (%)			
1	0.90	0.93	7.82	0.50	0.53	106
				1.00	1.01	101
2	0.91	0.92	4.26	0.50	0.50	100
				1.00	1.00	100
3	0.59	0.60	6.36	0.50	0.50	100
				1.00	1.01	101

[a] H_2O_2 disinfectant from three different manufacturers.
[b] Average value from five determinations.
[c] R.S.D. was the relative standard deviation of the five measurements by the prepared sensor.

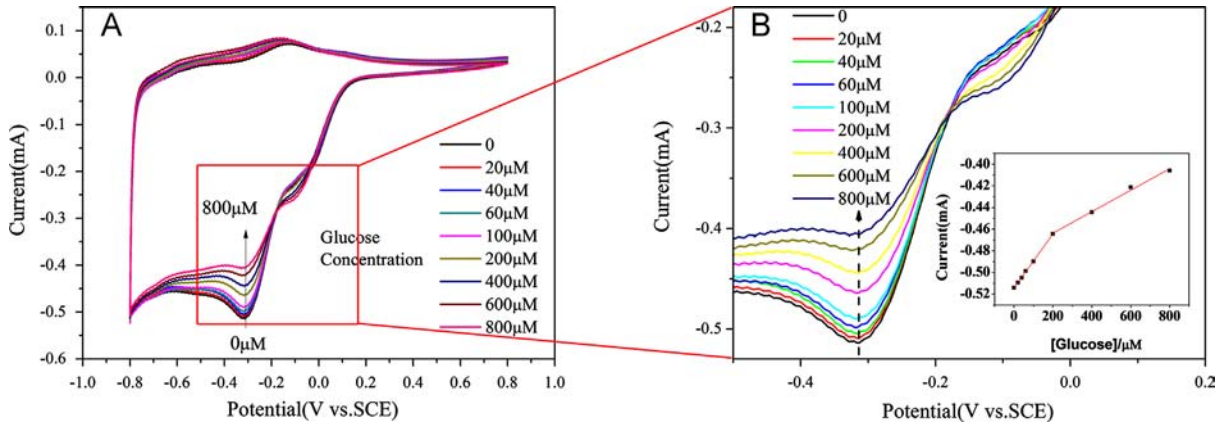

Fig. 5. (A) CVs of the GOx–AgNPs/TiO_2NTs electrode in 0.1 M of air-saturated PBS solution (pH 7.4) with different glucose concentrations. (B) Enlarged graph showing the rectangular region marked in (A). Inset of (B): the calibration plot of the cathodic current versus the glucose concentration at −0.31 V. Scan rate: 50 mV s^{-1}.

Acknowledgments

We would express our sincere thanks to the financial support from the National Natural Science Foundation of China (Grant nos.20927007 and 21075083) and Doctoral Program Foundation of Institutions of Higher Education of China (20120181120075) is gratefully acknowledged. Yanshu Jiang and Baozhan Zheng contributed equally to this work.

Appendix A. Supporting information

Supplementary data associated with this article can be found in the online version at http://dx.doi.org/10.1016/j.talanta.2013.03.015.

References

[1] R.A. de Abreu Franchini, C.F. de Souza, R. Colombara, M.A. Costa Matos, R.C. Matos, J. Agric. Food. Chem. 55 (2007) 6885–6890.
[2] R.K. Gilpin, L.A. Pachla, Anal. Chem. 77 (2005) 3755–3770.
[3] D. Vione, V. Maurino, C. Minero, D. Borghesi, M. Lucchiari, E. Pelizzetti, Environ. Sci. Technol. 37 (2003) 4635–4641.
[4] Y. Wang, J. Huang, C. Zhang, J. Wei, X. Zhou, Electroanalysis 10 (1998) 776–778.
[5] I.L. de Mattos, L. Gorton, T. Ruzgas, Biosensors Bioelectron. 18 (2003) 193–200.
[6] R.A. Potyrailo, V.M. Mirsky, Chem. Rev. 108 (2008) 770–813.
[7] P. Karam, L.I. Halaoui, Anal. Chem. 80 (2008) 5441–5448.
[8] A.A. Karyakin, E.A. Puganova, I.A. Budashov, I.N. Kurochkin, E.E. Karyakina, V.A. Levchenko, V.N. Matveyenko, S.D. Varfolomeyev, Anal. Chem. 76 (2003) 474–478.
[9] C. Chen, C. Sun, Y. Gao, Electrochem. Commun. 11 (2009) 450–453.
[10] X.S. He, C.G. Hu, H. Liu, G.J. Du, Y. Xi, Y.F. Jiang, Sens. Actuators B 144 (2010) 289–294.
[11] M.P.N. Bui, X.H. Pham, K.N. Nan, C.A. Li, Y.S. Kim, G.H. Seong, Sens. Actuators B 150 (2010) 436–441.
[12] Y. Li, J. Zhang, H. Zhu, F. Yang, X. Yang, Electrochim. Acta 55 (2010) 5123–5128.
[13] S. Wu, H. Zhao, H. Ju, C. Shi, J. Zhao, Electrochem. Commun. 8 (2006) 1197–1203.
[14] J. Huang, D. Wang, H. Hou, T. You, Adv. Funct. Mater. 18 (2008) 441–448.
[15] C.-Y. Lin, Y.-H. Lai, A. Balamurugan, R. Vittal, C.-W. Lin, K.-C. Ho, Talanta 82 (2010) 340–347.
[16] C.M. Welch, C.E. Banks, A.O. Simm, R.G. Compton, Anal. Bioanal. Chem. 382 (2005) 12–21.
[17] H. Chen, Z. Zhang, D. Cai, S. Zhang, B. Zhang, J. Tang, Z. Wu, Talanta 86 (2011) 266–270.
[18] K. Cui, Y.H. Song, Y. Yao, Z.Z. Huang, L. Wang, Electrochem. Commun. 10 (2008) 663–667.
[19] W. Zhu, X. Liu, H. Liu, D. Tong, J. Yang, J. Peng, J. Am. Chem. Soc. 132 (2010) 12619–12626.
[20] M.G. Hosseini, M. Faraji, M.M. Momeni, Thin Solid Films 519 (2011) 3457–3461.
[21] P. Si, S. Ding, J. Yuan, X.W. Lou, D.-H. Kim, ACS Nano 5 (2011) 7617–7626.
[22] X. Chen, S.S. Mao, Chem. Rev. 107 (2007) 2891–2959.
[23] F. Zhang, N. Guan, Y. Li, X. Zhang, J. Chen, H. Zeng, Langmuir 19 (2003) 8230–8234.
[24] W. Dong, S. Feng, Z. Shi, L. Li, Y. Xu, Chem. Mater. 15 (2003) 1941–1943.
[25] G. Guo, B. Yu, P. Yu, X. Chen, Talanta 79 (2009) 570–575.
[26] J. Li, J. Xu, W.-L. Dai, K. Fan, J. Phys. Chem. C 113 (2009) 8343–8349.
[27] M. Li, M.E. Noriega-Trevino, N. Nino-Martinez, C. Marambio-Jones, J. Wang, R. Damoiseaux, F. Ruiz, E.M.V. Hoek, Environ. Sci. Technol. 45 (2011) 8989–8995.
[28] B.-L. He, B. Dong, H.-L. Li, Electrochem. Commun. 9 (2007) 425–430.
[29] M. Sun, W. Fu, H. Yang, Y. Sui, B. Zhao, G. Yin, Q. Li, H. Zhao, G. Zou, Electrochem. Commun. 13 (2011) 1324–1327.
[30] A. Serra, M. Re, M. Palmisano, M. Vittori Antisari, E. Filippo, A. Buccolieri, D. Manno, Sens. Actuators, B 145 (2010) 794–799.
[31] P.-G. Su, Y.-P. Chang, Sens. Actuators, B 129 (2008) 915–920.
[32] J.X. Li, L.X. Yang, S.L. Luo, B.B. Chen, J. Li, H.L. Lin, Q.Y. Cai, S.Z. Yao, Anal. Chem. 82 (2010) 7357–7361.
[33] Y. Lai, H. Zhuang, K. Xie, D. Gong, Y. Tang, L. Sun, C. Lin, Z. Chen, New J. Chem. 34 (2010) 1335–1340.
[34] X. Liu, Z. Liu, S. Hao, W. Chu, Mater. Lett. 80 (2012) 66–68.
[35] I. Zhitomirsky, Adv. Colloid Interface Sci. 97 (2002) 279–317.
[36] Z. Hosseini, N. Taghavinia, N. Sharifi, M. Chavoshi, M. Rahman, J. Phys. Chem. C 112 (2008) 18686–18689.
[37] C. Noberi, A.C. Zaman, C.B. Üstündağ, F. Kaya, C. Kaya, Mater. Lett. 67 (2012) 113–116.
[38] H. He, W. Cai, Y. Lin, B. Chen, Langmuir 26 (2010) 8925–8932.
[39] W. Chanmanee, A. Watcharenwong, C.R. Chenthamarakshan, P. Kajitvichyanukul, N.R. de Tacconi, K. Rajeshwar, J. Am. Chem. Soc. 130 (2007) 965–974.
[40] P.L. Redmond, A.J. Hallock, L.E. Brus, Nano Lett. 5 (2004) 131–135.
[41] E. Jang, E.-K. Lim, J. Choi, J. Park, Y.-J. Huh, J.-S. Suh, Y.-M. Huh, S. Haam, Cryst. Growth Des. 12 (2011) 37–39.
[42] Y. Chen, X. Ji, X. Wang, J. Cryst. Growth 312 (2010) 3191–3197.
[43] J.Y. Du, N.N. Wei, X. Xin, J.L. Li, Biosensors Bioelectron. 26 (2011) 3602–3607.
[44] X. Shu, Y. Chen, H. Yuan, S. Gao, D. Xiao, Anal. Chem. 79 (2007) 3695–3702.
[45] L. Chen, L. Lu, Y. Mo, Z. Xu, S. Xie, H. Yuan, D. Xiao, M.M.F. Choi, Talanta 85 (2011) 56–62.
[46] T. Rajh, L.X. Chen, K. Lukas, T. Liu, M.C. Thurnauer, D.M. Tiede, J. Phys. Chem. B 106 (2002) 10543–10552.
[47] S. Yonghai, et al., Nanotechnology 20 (2009) 105501.
[48] W.B. Lu, Y.L. Luo, G.H. Chang, X.P. Sun, Biosensors Bioelectron. 26 (2011) 4791–4797.
[49] Q.Y. Cai, X.Y. Pang, D.M. He, S.L. Luo, Sens. Actuators B 137 (2009) 134–138.